



Energy harvesting and strain sensing in smart tire for next generation autonomous vehicles



Deepam Maurya^{a,b,*,1}, Prashant Kumar^{a,1}, Seyedmeysam Khaleghian^c, Rammohan Sriramdas^a, Min Gyu Kang^a, Ravi Anant Kishore^a, Vireshwar Kumar^d, Hyun-Cheol Song^e, Jung-Min (Jerry) Park^d, Saied Taheri^{f,*}, Shashank Priya^{a,b,*}

^a Bio-inspired Materials and Devices Laboratory (BMDL), Center for Energy Harvesting Materials and Systems (CEHMS), Virginia Tech, Blacksburg, VA 24061, United States

^b Institute for Critical Technology and Applied Science (ICTAS), Virginia Tech, Blacksburg, VA 24061, United States

^c Department of Engineering Technology, Texas State University, San Marcos, TX 78666, United States

^d Department of Electrical and Computer Engineering, Virginia Tech, Blacksburg, VA 24061, United States

^e Center for Electronic Materials, Korea Institute of Science and Technology (KIST), Seoul 02792, Republic of Korea

^f Center for Tire Research (CenTiRe), Virginia Tech, Blacksburg, VA 24061, United States

HIGHLIGHTS

- Developed high energy density harvester-cum-sensor to power wireless data transfer.
- The generated energy from tire strain harvester was enough to directly power 78 LEDs.
- A mathematical model for tire-road interaction and piezoelectric response.
- Real environment test for sensing tire-road interaction under different variables.
- Demonstrated the self-powered smart tire sensor for autonomous vehicles.

ARTICLE INFO

Keywords:

Energy harvesting
Piezoelectric sensor
Smart tires

ABSTRACT

We demonstrate the feasibility of the strain energy harvesting from the automobile tires, powering wireless data transfer with enhanced frame rates, and self-powered strain sensing. For this, we used a flexible organic piezoelectric material for continuous power generation and monitoring of the variable strain experienced by a tire under different driving conditions. Power output of $\sim 580 \mu\text{W}$ at 16 Hz ($\sim 112 \text{ km/h}$) from the energy-harvester and mounted on a section of a tire, is sufficient to power 78 LEDs. We further demonstrate that the stored energy was sufficient to power the wireless system that transmits tire deformation data with an enhanced frame rate to control system of a vehicle. Using sensors mounted on a tire of a mobile test rig, measurements were conducted on different terrains with varying normal loads and speeds to quantify the sensitivity and self-powered sensing operation. These results provide a foundation for self-powered real-time sensing and energy efficient data transfer in autonomous vehicles.

1. Introduction

In autonomous vehicles, energy requirement has been increasing rapidly with the increased number of onboard sensors, and the requirement for an increased rate of wireless data transfer for safe and reliable driving. There is tremendous development taking place in both

academia and industry to provide devices, systems, and techniques [1,2] that lead to energy efficient self-governing automobile environment [3,4]. For automobiles, tires act as an interface between the vehicle control system and the external environment. The abundant vibration and strain energy in a rolling tire can be used for energy harvesting to power wireless sensors [5]. This is especially important

* Corresponding authors at: Bio-inspired Materials and Devices Laboratory (BMDL), Center for Energy Harvesting Materials and Systems (CEHMS), Virginia Tech, Blacksburg, VA 24061, United States (D. Maurya and S. Priya).

E-mail addresses: mauryad@vt.edu (D. Maurya), staheri@vt.edu (S. Taheri), spriya@vt.edu (S. Priya).

¹ These authors contributed equally to this work.

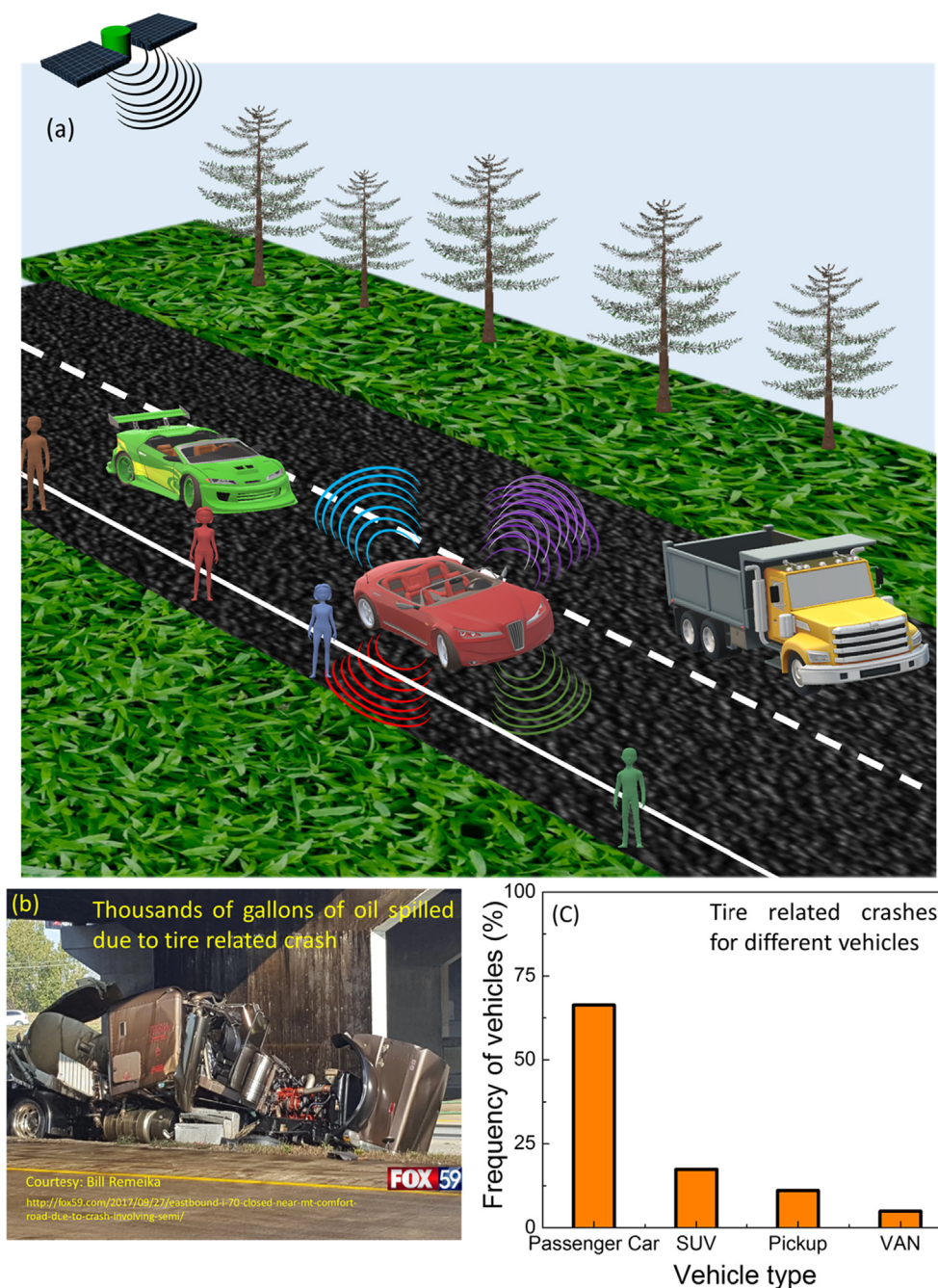


Fig. 1. (a) Schematic of an autonomous vehicle on the road. (b) Oil spill due to a flat tire-related accident causing serious environmental threat. (c) The distribution (%) of tire-related crash vehicles including their types. (Source: U.S. Department of Transportation, National Highway Traffic Safety Administration).

considering the increasing length of the wires with the number of sensors in modern cars, which further increases weight of the vehicle, needs more space, and reduces vehicle’s reliability [6]. Such energy harvesting solutions will ultimately reduce the load on the vehicles’s main battery, thereby, increasing the efficiency of the vehicle. In order to achieve tire-based self-powered sensing of the external environment and wireless data transfer, recent focus has been on developing smart tires with energy generation capability [7,8]. The sensor arrays, in smart tires, are used for monitoring and evaluating different physical quantities such as road/terrain characteristics, air pressure, road/tire friction, loadings, wear, and hydroplaning [9]. These quantities are then used by intelligent algorithms for enhancing the consistency, longevity, safety, stability and fuel efficiency of a vehicle [7,10,11]. The smart tires equipped with the efficient energy harvesting systems, are

not only beneficial for the autonomous cars (Fig. 1(a)), but, also will be helpful in controlling tire-related crashes in traditional vehicles. The tire-related crashes can be extremely deadly, and sometimes highly damaging to the environment, as shown in Fig. 1(b). According to a report [12], out of the total number of crashes, the tire-related crashes were approximately 6%, 4.6%, 4.3%, and 3.5% for passenger cars, SUVs, pickups, and vans, respectively. Among different kinds of vehicles, the tire-related crashes (as shown in Fig. 1(c)) were highest for the light passenger car (66.3%), which was followed by SUVs (17.4%), pickups (11.1%), and vans (4.9%). Therefore, developing an energy efficient smart tire has been one of the important aspects in achieving fully autonomous vehicles. Global initiatives such as European Union project APOLLO (2003) and Bridgestone/Firestone recall helped to fuel the momentum of intelligent and energy efficient tire development in

the beginning of 21st century [13,14]. During initial stages of research, the main focus was to develop the tire pressure monitoring system (TPMS) [15,16]. However, recent studies have shown that other characteristics such as road friction, tire-road interactions, and wheel loads are equally important to ensure better and safe driving [7,8,11,17,18].

Different methods, such as accelerometers [11,19], piezo-based [20,21], magnetic-based [17,22,23], capacitive-type [24,25], and surface acoustic wave (SAW) [26,27], have been described in previous studies to measure the parameters such as acceleration, strain, temperature, and pressure. All these technologies have their advantages and limitations with respect to tire platform. For example, accelerometers are easy to integrate and can work over a wide range of temperature, however, they are rigid, expensive, not compatible with large deformations, and extremely sensitive to the surrounding noise [7]. Capacitive sensors are good candidates for pressure sensing and strain measurements [25,28], but suffer from the drawback that their sensitivity varies with temperature and hence require additional compensation circuits [7]. Pohl et al. used SAW technique to estimate the tire deformations and frictional characteristics [29], however, this method often needs additional acquisition systems, wireless communication infrastructure, passive external power, and may have difficulty to withstand large deformation of a tire [10,30]. Most of these embedded sensors require a robust wireless infrastructure along with the power source. For example, TPMS [16,31], which is integrated in each wheel to monitor the tire pressure, usually, consists of a pressure sensor, a microcontroller for processing, a radio frequency (RF) communication system to wirelessly transmit the data to the vehicle's central receiving unit, and a battery as a power source. This scenario is expected to become more complex with the increasing number of sensors in the next generation of the autonomous vehicles [32]. Enhanced number of sensors require additional power, which further depends on the rate of the data transfer. Although batteries are the easy and inexpensive source for providing constant voltage supply, they have a major drawback of their limited utilization time, and high labor cost for replacement [8,33]. The limited availability of energy restricts the use of increased frame rate for the wireless data transfer, which renders reduced reaction time for the driver in case of an emergency.

To replace these batteries, various energy harvesting technologies have been developed for harnessing the untapped mechanical energy of tire to electricity, which otherwise goes waste. Most of the vehicle-related energy harvesting technologies are focused on vehicle vibration and/or exhaust heat with the aim of reducing the dependency on the vehicle's main heavy battery and extra load on the engine [6,34]. Some of these methods of tire energy harvesting utilize transduction such as: electromagnetic [35,36], piezoelectric [16,33], microfiber/piezoelectric composites [30,37,38], and nanogenerators (based on triboelectric and Zinc Oxide (ZnO)) [39,40]. However, most of these harvesters had certain limitations. For example, electromagnetic harvesters are cost-effective, but difficult to integrate due to their large size. Furthermore, MFCs and nanogenerators are flexible in nature and may exhibit reasonable power density. However, the fabrication process of these materials is complex, expensive, and they don't exhibit enough output power. The integration of these sensors would dramatically increase the cost of the tire. Additionally, because these harvesters are very sensitive to the temperature, the increased tire temperature during motion could be an issue [37]. The resonance based PZT harvesters are not able to function beyond the certain frequency ranges and required tip masses, making the system bulky to integrate in a tire. On the other hand, flexible PVDF based harvester are good match for harvesting tire strain energy considering large deformation of tires and ease in integration. In order, to achieve cost-effective and robust intelligent tires, one needs to develop an effective self-powered sensing method, which does not depend on the external power source. The sensing element should be easy to integrate within tire to avoid complexity and possess low stiffness [7,8]. These flexible sensors should have stable behavior as a function of temperature with low fatigue.

In present work, we provide a cost-effective solution to above mentioned issues and demonstrate a self-powered sensor based upon an organic piezoelectric material. A low value of elastic modulus ensures the high strain development in this piezoelectric patch, which is one of the important parameters for strain sensors. We realized the high-power density and high temperature (up to 90 °C) stability of organic piezoelectric based harvester. Further, we demonstrate that the generated energy from this piezoelectric patch, in normal tire condition, is sufficient to power 78 LEDs and wireless systems. This provides an estimate for the power needed to develop efficient wireless data transfer and power management. In order to understand the dynamics of the tire during rotation under load, we developed a mathematical model and evaluated various key parameters such as radial and tangential displacement of the tire, and voltage from a flexible piezoelectric sensor. Based upon the mathematical analysis, we integrated piezo patch in a tire mounted in a mobile test rig. The tests were performed on different types of roads (under variable wheel loading) to demonstrate the sensing capabilities. These experimental results were also validated qualitatively (voltage trend with velocities) through analytical modeling.

2. Experimental

In order to measure the strain in the tire and for their health monitoring, the piezoelectric material was used. First, to assess the power requirements, we mounted a PVDF based piezoelectric patch (KF Piezo film, KUREHA) on a section of the tire. The list of properties for this material has been provided in the [supplementary information \(Table S1\)](#). The tire-section was rigidly secured at two ends to provide the cantilever boundary condition on a vibration isolation smart table (Newport ST series). The shaker, which was coupled with a function generator through an amplifier (HP 6826A), was used to excite the tire-section. The output voltage was measured using an oscilloscope (DSO1014A, Keysight). The 2D scanning laser vibrometer (Polytec PSV-500) was used to measure the displacement and the dynamic profile of tire-section in a lab environment. Furthermore, we conducted the experiments to evaluate the thermal stability and reversibility of the functional response of piezoelectric patch. A heat gun was used to heat the system, and the temperature was measured through a K-type thermocouple. During tapping on the tire (through a shaker), we tried to emulate the real displacement profile of a moving tire in the lab environment. Furthermore, we demonstrated powering of 78 LEDs, and the capability of the wireless data transfer from a sensor (MIDASCON) using energy stored from the piezoelectric patch integrated on a tire-section. Lastly, we mounted our sensor on the real tire (Goodyear, model # P245/70R17) installed on a mobile tire test rig. These field tests were performed using different normal loads and speeds at Virginia Tech Transport Institute (VTTI).

3. Results and discussion

Fig. 2(a) shows the schematic of the tire deformation during motion of a typical vehicle. Please note three zones of the tire deformation; A and C are compressive zones, and B is the tensile zone. During motion on a given terrain, the deformation of the tire generates a waveform sensed through a self-powered piezoelectric sensor. This waveform is schematically shown in Fig. 2(b) [37]. Using our piezoelectric based self-powered sensor, mounted on the tire, we experimentally observed similar waveform due to tire deformation. The waveform characteristics are a function of varying load depending upon vehicle, speed, and terrain etc. PVDF based organic piezoelectric materials are an excellent choice here because of a wide frequency range of operation, sensitivity (Fig. 2(d)), and small Young's modulus (Fig. 2(e)). Further, this polymer-based piezoelectric material is stable up to 90 °C (Fig. S1(a)), which meets the requirement for mounting within a tire.

In order to characterize the voltage output characteristics of the piezoelectric sensor, mechanical excitation from a shaker was utilized.

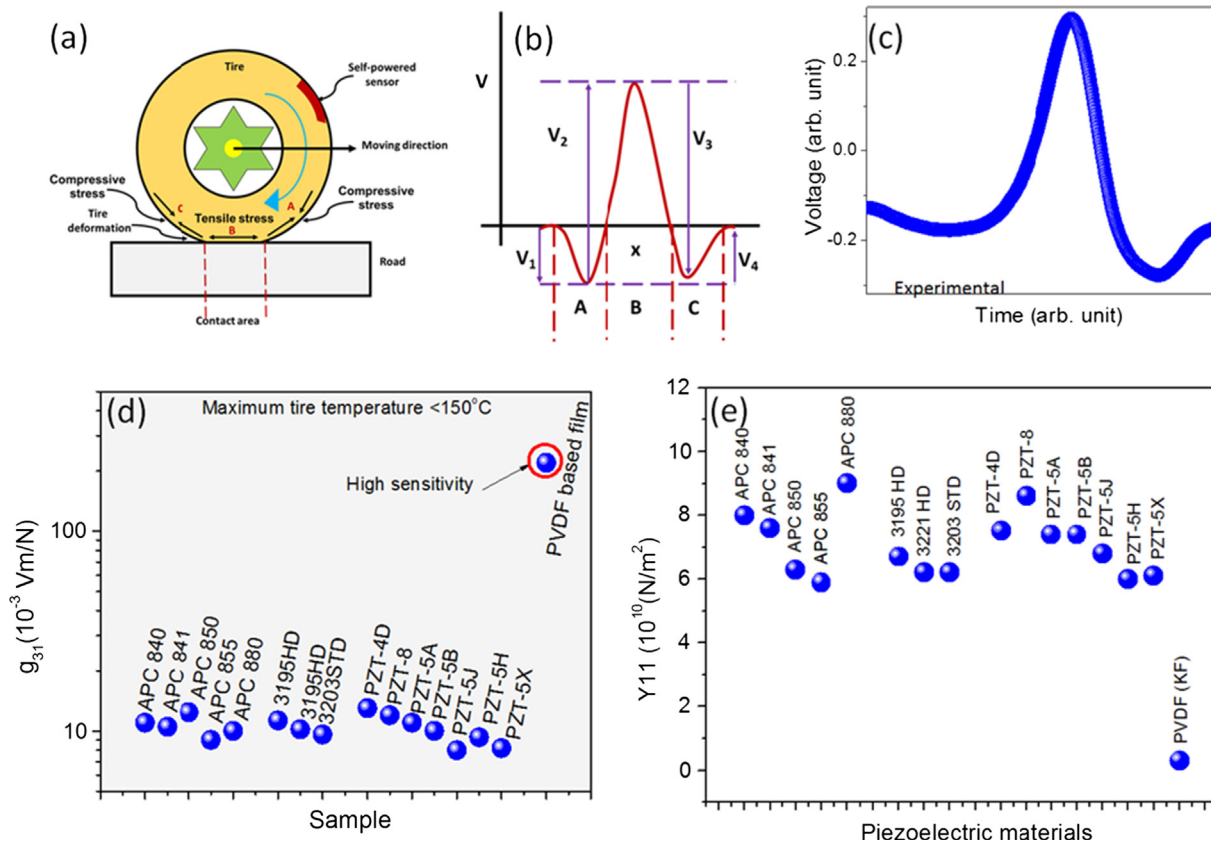


Fig. 2. (a) Schematic of the tire deformation with different types of strain. (b) Schematic waveform generated due to the tire deformation. (c) Experimental waveform due to the tire deformation. (d) Voltage coefficient of various piezoelectric materials. (e) Young's modulus of various piezoelectric elements.

Fig. 3(a) shows a photograph of the sensor mounted on a section of a tire, where shaker is behind this tire-section. The dynamics of the piezoelectric sensor, on such excited tire-section, was investigated using a laser vibrometer. Tire section was discretized into many points, which were scanned through a laser. The root mean square (RMS) displacement profile, during one of the measurement, can be seen in Fig. 3(b). This profile shows almost a flat dynamic response (each point has the same displacement) across the scanned area of the tire-section, which illustrate that the tire-section was systematically excited with no relative motion among various points on the surface at a given frequency. These results were used to emulate the dynamics of a tire in a real moving vehicle, when a particular section of a tire gets a repetitive normal reaction force from the road after a regular interval of time (or at a particular frequency). Fig. 3(c) shows the displacement at the center point of the tire section. We have calculated the strain values across the tire section by using the displacement profile (as input) measured at the center of the patch (Fig. 3(d)). Corresponding to the displacement of 2 mm at 16 Hz, a 0.8% maximum strain was estimated for one cycle. During vehicle movement for a long period of time and then applying brakes, could sometimes heat-up tires to the temperatures ~80–90 °C [37], which requires sensors to be stable in that temperature regime. Fig. 3(d) shows the peak to peak voltage at variable temperatures. The piezoelectric sensor used in this work was found to exhibit stable voltage output over a temperature range of 25–90 °C. From the results under a given thermal cycle, one can infer that the sensor was stable up to 90 °C and did not exhibit hysteresis losses due to thermal cycling. It is worthwhile to mention, we tested the piezoelectric patch under controlled mechanical excitation at 16 Hz for 3 days, and did not observe any significant change in the patch output, as shown in Fig. S1(b).

3.1. Electrical characterization in lab environment

We measured the voltage output from the piezoelectric patch under different displacements at various frequencies (7–16 Hz). The frequency range was derived from the vehicle's speed (48–112 km/h) considering average tire dimensions (overall diameter- 0.63 m). One can clearly observe in Fig. 4(a)–(e) increase in the open circuit voltage (OCV) output with increasing displacement at the center of the patch. Increased displacement enhances the strain in the tire, which in turn, results in enhanced voltage output. Fig. 4(f) shows the summary of voltage output as a function of frequency at different displacements. The output voltage was found to increase monotonously with increasing frequency for displacements up to 1.5 mm. However, for displacements > 1.5 mm, the output voltage was found to decrease with increasing frequency. The voltage-frequency response indicated that the resonance frequency of our experimental system doesn't fall within the given frequency range. This provided us an opportunity to conduct the systematic study on the tire (which should represent the real case as well), in a laboratory environment. Power generation for two different cases was quantified: (i) fixed tire displacement (2 mm) with varying frequencies, and (ii) fixed shaker power input at varying frequencies.

In order to measure maximum instantaneous power generated from the piezoelectric patch, at 2.0 mm displacement, a range of the load resistances was utilized, as shown in Fig. 5(a). The maximum power was obtained to be 150 μW at a frequency of 16 Hz across 2 MΩ load resistance. We also measured the power output at various other frequencies using the same experimental setup (at 2 mm displacement), and found that the peak power range varied from 100 μW to 150 μW. On further increasing the input voltage amplitude for the shaker, the maximum power was obtained to be 580 μW (Fig. 5(b)). Fig. 5(c) shows the open circuit voltage generated at different frequencies for a fixed shaker amplitude. With increasing frequency, the output voltage was

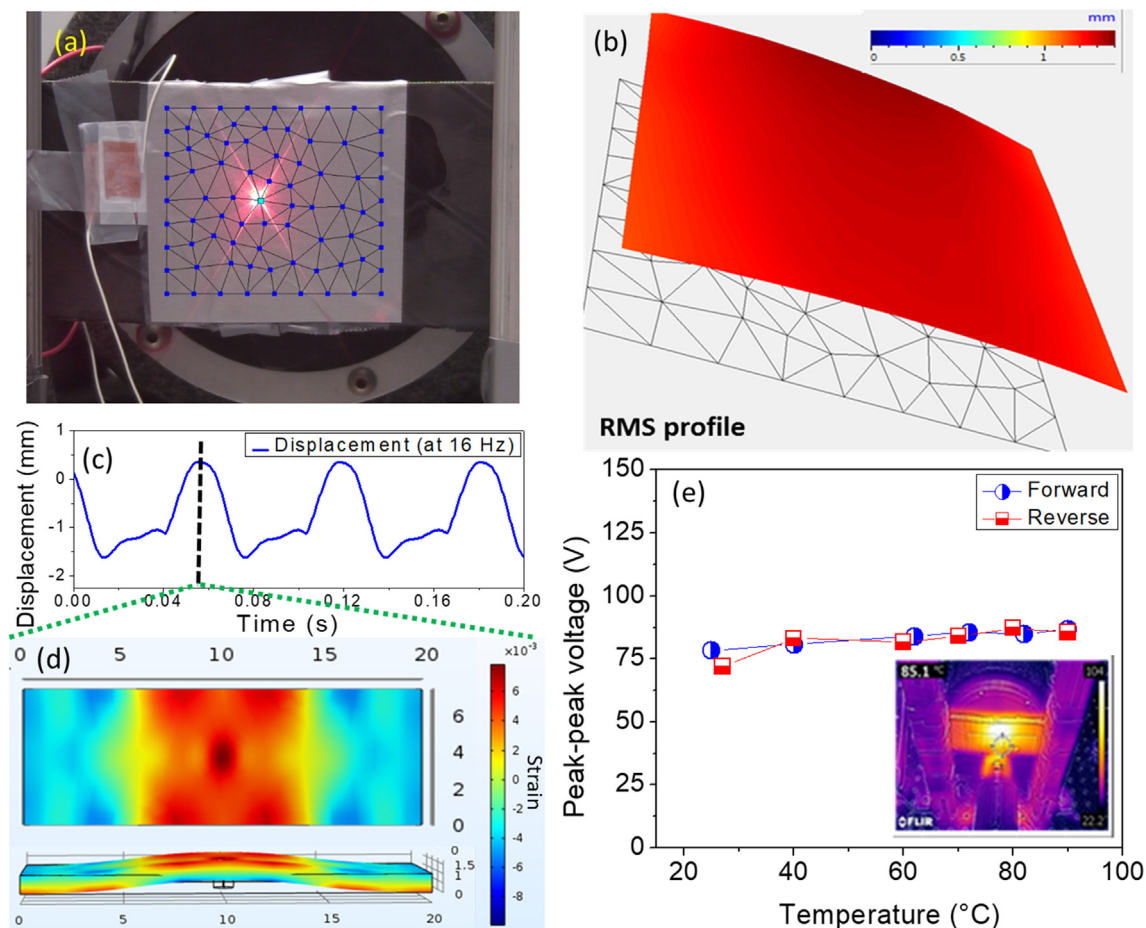


Fig. 3. (a) Photograph of the laser scanning path for measuring displacement. (b) Surface displacement measured using laser vibrometer. (c) Displacement at the center point of tire section. (d) Simulated maximum strain contour for the displacement input shown in Fig. 3(c). (e) Performance of organic piezoelectric patch at different temperatures. Inset image shows an infrared camera photograph indicating temperature distribution.

found to increase up to 13 Hz before slightly dropping at 16 Hz. Fig. 5(d) shows the force input of shaker to the tire setup. The force measurements were carried out using a Futek force sensor having a sensitivity of 48.6 Newton/Volt (Fig. S2). It can be observed that there is a significant difference in the force dynamics (at variable frequencies) at different excitation input. This force difference can be easily observed in power output as well. On increasing the shaker input, although tire displacement saturated, force input to the tire was found to increase (as shown in Fig. 5(d)) significantly, thereby, increasing the voltage and power output.

This harvester-cum-sensor patch can have multiple functions, because, it can sense tire dynamics, and provide power for wireless data transfer. Fig. 6(a) shows the setup for the successful demonstration of lighting 78 LEDs directly using the power generated from this piezoelectric patch. To demonstrate real applications of the power generated, we powered a commercial wireless sensor using stored power (in a capacitor) through a rectifier circuit (Fig. S3) from the piezoelectric patch, and demonstrated wireless data transfer related to the temperature and humidity, as shown in Fig. 6(b). The data transfer was accomplished using a commercial wireless sensor (installed on an electric kettle) and a mobile phone based app. Fig. 6(c) illustrates the temperature and humidity information from the surface of a kettle with respect to time. After switching on the kettle, the surface temperature increased, which, in turn, made the surrounding ambient dry reducing humidity. This demonstration shows the capability of this piezoelectric patch as a sensor to read the real-time information without external bias, and powering the onboard wireless data transfer system to transmit the sensed information. Next, we discuss the power

management for this wireless data transfer.

3.2. Power management for the wireless data transfer

In a TPMS system, the communication system regularly sends message frames containing tire pressure information. If the tire pressure is below a threshold, the central receiving unit presents an alert on the driver’s dashboard. In a TPMS, most of the battery’s power is consumed during transmission of the message frames [41]. Hence, to conserve energy and extend battery life, the frame rate transmitted from the TPMS is traditionally limited to a very low value, e.g., the communication system transmits only one frame per minute [42]. Note that the transmission of a message frame only lasts for a few milliseconds, and the communication system remains idle for the rest of the time to conserve energy. This reduces drivers’ precious reaction time in case of the tire blowout or sudden puncture, which could lead to an accident. Further, the wireless communication system in traditional TPMS cannot support a large amount of data transfer, and hence the data is limited to the minimal information related to tire pressure. The communication of additional information about other important characteristics, such as road friction and tire-road interactions, require more advanced communication systems, such as Bluetooth and Wi-Fi. Fig. 6(d) exhibits the power required for the wireless data transfer for the different number of transmitted frames per minute in different state-of-the-art technologies. These plots show increased power requirement for highly efficient data transfer rate in technologies like Bluetooth and Wi-Fi as compared to TPMS. Therefore, advanced wireless data transfer technologies require more power, increasing the load further on the available energy.

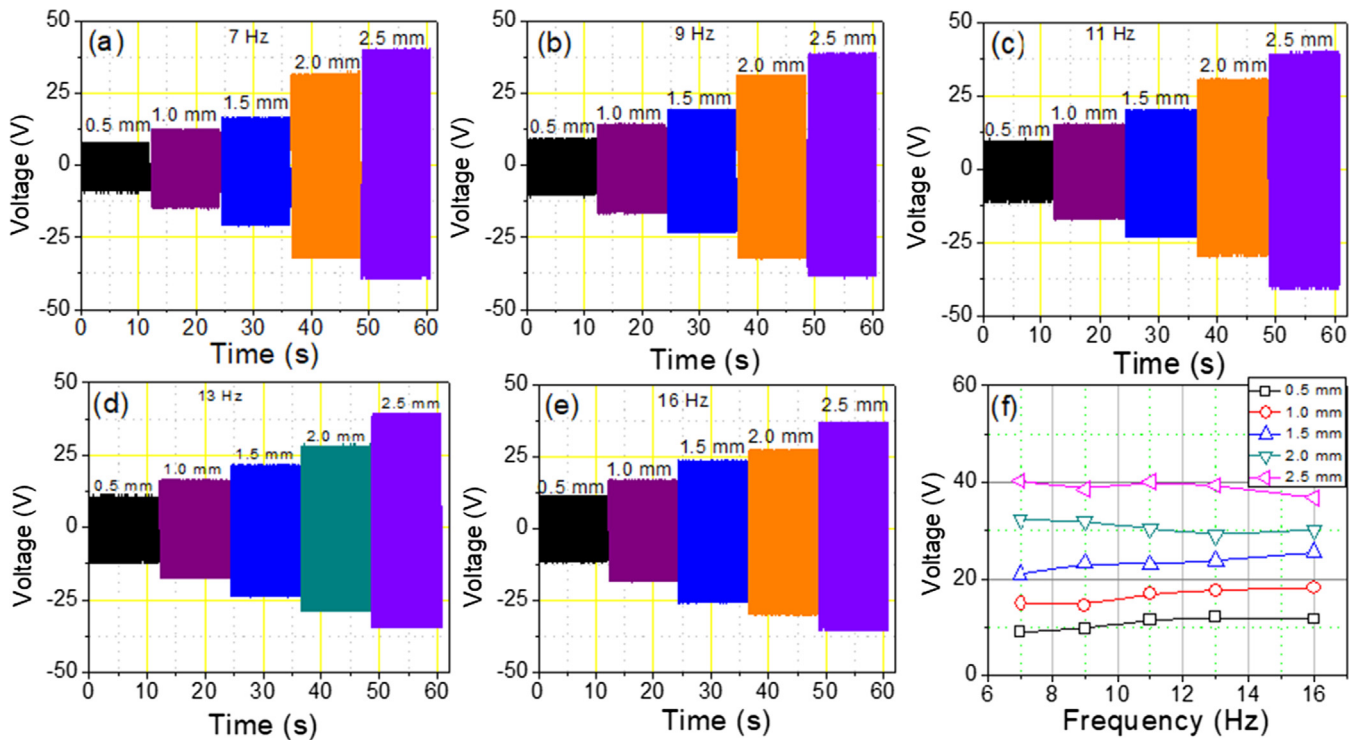


Fig. 4. Output voltage at different displacements for (a) 7 Hz, (b) 9 Hz, (c) 11 Hz, (d) 13 Hz, (e) 16 Hz. (f) Output voltage versus frequency at different displacements. The displacements were measured at the center point of tire section.

Here, we analyze the frame rate that could be achieved by our self-powered sensor fitted with a state-of-art Bluetooth Low Energy (BLE) communication system [43]. This communication system requires around 4 ms to transmit one message frame which comprises of monitoring information of 512 bits [44]. On average, the communication system draws around 40 mW at 3 V during this transmission. Hence, a

total of 160 μ J is required to transmit a frame. A detailed transmission process is shown in Table S2. With an average power generation of around 225 μ W in our self-powered sensor, the required energy can be generated and stored in one second. Hence, our self-powered sensor is capable of sending at least one frame per second (60 frames per minute). From the above analysis, we observe two advantages of using

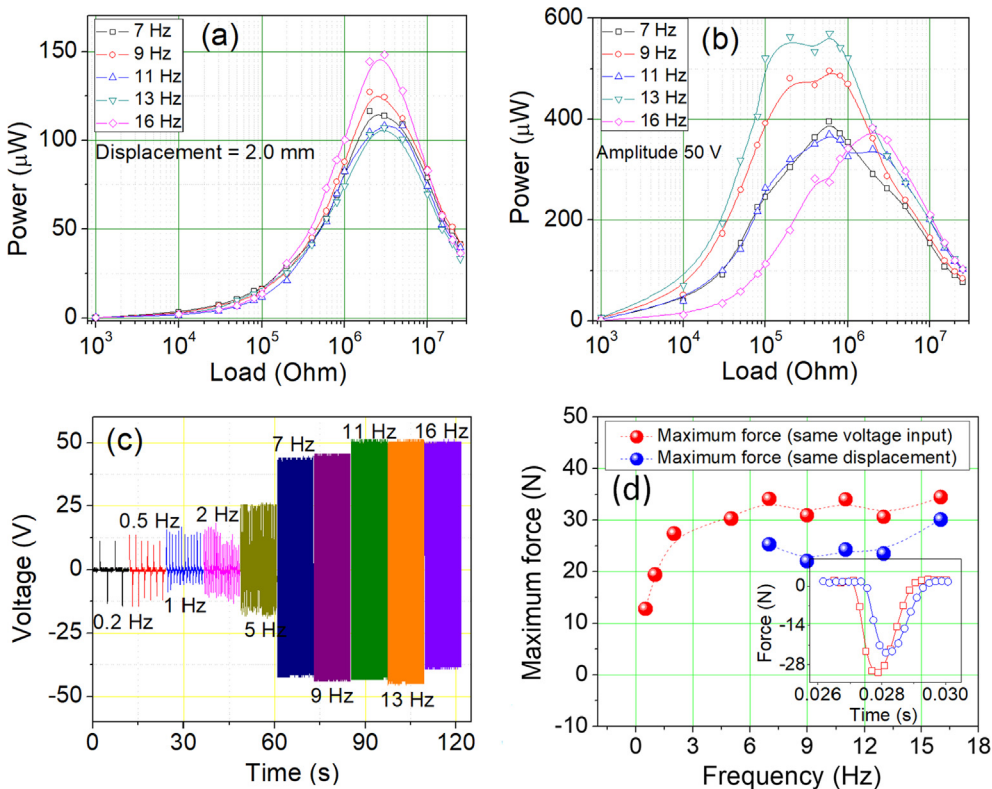


Fig. 5. (a) Power output versus resistance at different frequencies at controlled displacements (measured at center point). (b) Power output at the increased level of shaker amplitude (50 V input) from the piezoelectric sensor. (c) Voltage output at different frequencies for an increased level of shaker amplitude selected in (b). (d) Force input to the tire from shaker at different frequencies. Inset image shows the waveform of the force applied by the shaker on the tire section.

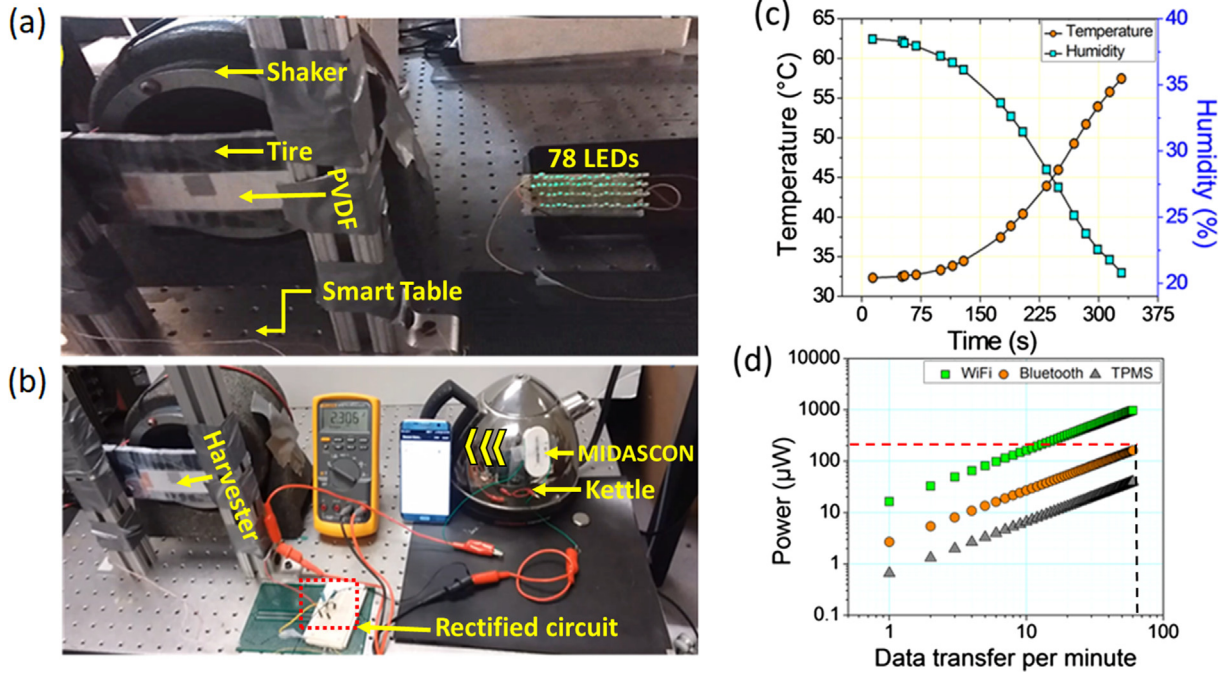


Fig. 6. (a) 78 LED were powered using the piezoelectric patch under consideration. (b) Wireless data transfer demonstration using power stored from the piezoelectric patch mounted on the tire section. (c) Temperature and humidity data transferred wirelessly by utilizing stored energy. (d) Power management analysis for various current technologies (Data sheets are included in supporting information). The dotted lines show the power ($\sim 225 \mu\text{W}$) requirement for data transfer (~ 60 data per minute).

our sensor. Firstly, we could utilize Bluetooth technology which supports the transfer of a larger amount of data as compared to the TPMS. Secondly, the achievable frame rate with our sensor could be two orders of magnitude higher than the conventional TPMS. The affordability of sending data with increased frame rate per minute provides increased critical reaction time to the driver to handle the situation in case of a tire blowout or puncture increasing road safety [45].

3.3. Tire modeling for field condition

After detailed experimental analysis in a lab environment, a theory has been developed to illustrate the integration of tire dynamics with our piezoelectric patch for the real road conditions to predict the voltage outcomes. In this section, through mathematical modeling, we predicted the displacements of a tire, the voltage output from a patch for different driving conditions such as tire speed.

3.3.1. Theory: Voltage response from an organic piezoelectric patch on a rotating tire

The voltage response from a PVDF based piezoelectric patch, mounted on a tire, was estimated from the electrical enthalpy density by applying Hamilton’s principle [46]. The electrical enthalpy density H , for a piezoelectric patch on a tire, defined by the domain Γ as a function of strain S_{11} , electric field E_3 , Young’s modulus c_{11} , permittivity ϵ , and piezoelectric stress coefficient e_{31} is given as:

$$H = \frac{1}{2} \int_{\Gamma} (c_{11}S_{11}^2 - 2e_{31}S_{11}E_3 - \epsilon E_3^2) d\Gamma, \tag{1}$$

The tire was modeled as a rotating ring with radial and tangential stiffness, as described in references [47–49]. The circumferential strain in the tire, S_{11} , can be written as a function of circumferential deflection, $v(\theta, t)$, as [50]

$$S_{11} = \frac{1}{2r^2} (v + v')^2 + \frac{z}{r^2} (v' + v''), \tag{2}$$

where r is the radius of the tire and z is the distance along the thickness.

It may be noted that the inextensible condition ($w = -v'$) was employed in deriving Eq. (2). Following the procedure developed by Meirovitch to estimate the response of gyroscopic systems [51], the radial deflection, w , can be given by

$$w(\theta, t) = \sum_{n=1}^{\infty} \frac{Fn^2 \cos(n(\theta - \phi_0 + \Omega t))}{\pi b(n\Omega(m_n n \Omega - g_n) - k_n)}, \tag{3}$$

where the force at an angle ϕ_0 , width, stiffness, mass, and damping of n th mode, and wheel rotation rate are denoted by F , b , k_n , m_n and g_n , and Ω respectively [48]. It was assumed that the piezoelectric patch would not affect the dynamics of tire motion. Hence, the voltage developed by the patch was determined by solving the following differential equation obtained by collecting the terms containing the first variation of voltage from the action integral.

$$\frac{V(t)}{R} - \theta_0 + C_p \dot{V}(t) + \frac{b_0 e_{31} (t + t_p)}{2r} (v'(\theta_0, t) + \dot{v}'(\theta_0, t)) = 0, \tag{4}$$

where b_0 , t , t_p and C_p are width, thickness of tire, piezoelectric patch spanning over an angle of θ_0 and film capacitance respectively.

3.3.2. Simulations

The tire model used in the experiments and simulations was P245/65R17 105S. Based on the experimental modal analysis, the equivalent radial and tangential stiffness were estimated to be 1562 kN/m^2 and 2212 kN/m^2 respectively. These numbers were obtained by matching first three tire resonant frequencies corresponding to $n = 2, 3$ and 4 with experimentally observed frequencies 93, 108 and 132 Hz, respectively. The radial displacement was estimated for a load of 3000 N at three speeds namely, 8 km/h, 16 km/h and 32 km/h. The piezoelectric patch had a width of 80 mm and spanned over an angle of 12° on the tire. The radial displacement and tangential displacement were estimated from Eq. (3), and are plotted in Fig. 7(a) and (b) respectively. It can be observed that both radial and tangential displacement amplitudes of the tire do not change with speed. However, the rate of change of the displacement was higher with increasing speed. The voltage developed by the piezoelectric patch was estimated by solving

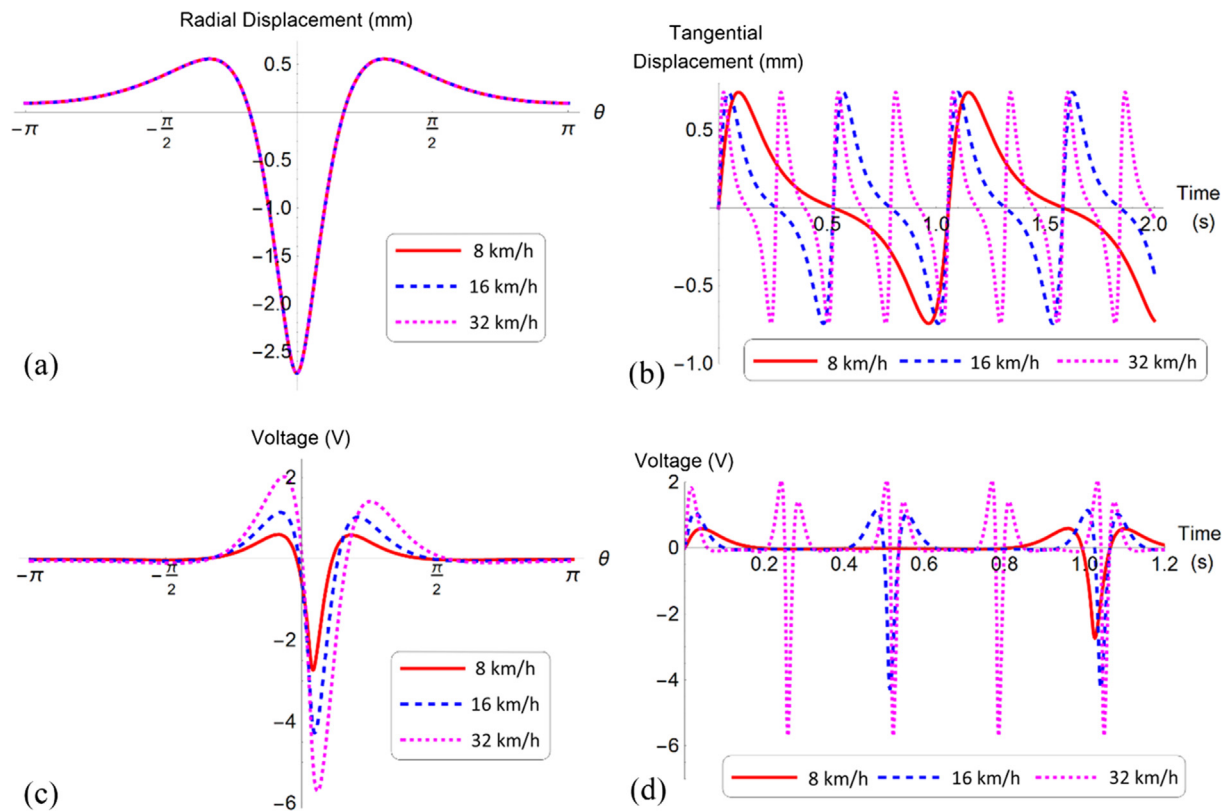


Fig. 7. (a) Radial displacement of the tire as a function of angular position at three different speeds of 8 km/h, 16 km/h, and 32 km/h. It can be noticed that the displacement remained same for all the speeds with respect to the angular position. (b) The tangential displacement as a function of angular position for three speeds. It can be observed that the amplitude of the displacement remains the same. However, the rate at which the displacement changes with time, increases with speed. (c) The voltage response as a function of angular position for three speeds. (d) The voltage developed by the piezoelectric patch at different speeds is shown as a function of time. Although the displacement of the tire was not increasing with speed, the generated voltage and the power was found to increase with speed.

the differential equation given in Eq. (4). The voltage developed by the piezoelectric patch at a load resistance of 100 kOhm for three different speeds is shown in Fig. 7(c) as a function of angular position. The voltage developed by the patch in a time domain is shown in Fig. 7(d). The RMS voltage at 8 km/h, 16 km/h, and 32 km/h speeds was 0.21 V, 0.62 V, and 1.1 V, respectively. The resulting average power at 8 km/h, 16 km/h, and 32 km/h speeds was 0.4 μ W, 3.8 μ W and 12 μ W, respectively. We performed simulations for different sensor patch length and found that the voltage output increases with the increase in the sensor patch length (Fig. S4). By arranging multiple piezoelectric patches along the tire, the generated power can be scaled up.

4. Real-time field testing of the sensor integrated within a tire

After characterizing the piezoelectric patch and performing the modeling, we mounted the patch on a tire (shown in video S1) integrated within a mobile test rig, as shown in Fig. 8(a). The tire was initially inflated to 193 kPa. The waveform due to tire deformation was measured using a piezoelectric sensor mounted inside the tire. The experiments were performed on different terrains such as asphalt and concrete mostly at the speed of 16 km/h, and normal loads of 3kN and 4kN. The waveform output is shown in Fig. 8(b)-(d). These results illustrate that under the same normal load and varying terrains, the voltage output from the piezoelectric patch remained almost same (Fig. 8(b)). This behavior can be explained as stress generated in the tire is proportional to radial acceleration, which remained unchanged for different terrain characteristics (under the same load). This leads to the unchanged voltage output waveform from the sensor.

In another parametric study during the field test, we observed that with increasing normal load on the tire, the voltage output was

decreased significantly. This phenomenon could be attributed to the redistribution of the stress at the tire-road contact area, under increased normal load (on the same path) [52]. This redistribution of stress led to a higher stress on the outer periphery (tire shoulder) of the tire-road contact area, reducing stress on the central part (tire crown), where the piezoelectric patch was attached. This resulted in reduced voltage output. In order to observe the effect of the speed, output waveform was measured at 16 and 32 km/h. The higher speed was found to result in the higher magnitude of the peaks in the output waveform (Fig. 8(e)). This phenomenon can be explained by considering the fact that with increasing velocity, the rate of change in displacement of the tire increases, which further increases the voltage output. This behavior was also modeled in our theoretical calculations. Magnified image of the waveform (Fig. 8(f)) clearly shows that our piezoelectric sensor-cum-harvester clearly captured the waveform of tire's compression and tension cycle. We have also performed additional field test under conditions like varying tire pressure, normal load, speed. The corresponding results have been added to the supplementary information (Fig. S5). Our experimental results are qualitatively in very good agreement with modeling results. The experimental voltage profile (compression-tension-compression) and trend of increasing voltage with an increase in tire speed (because strain rate of tire-patch increases as explained in modeling section) are consistent with modeling predictions. These results clearly indicate the effect of external variables on the sensor output and their effect on the tire dynamics, which can be used for sensing terrain characteristics, tire pressure, normal load, and vehicle speed.

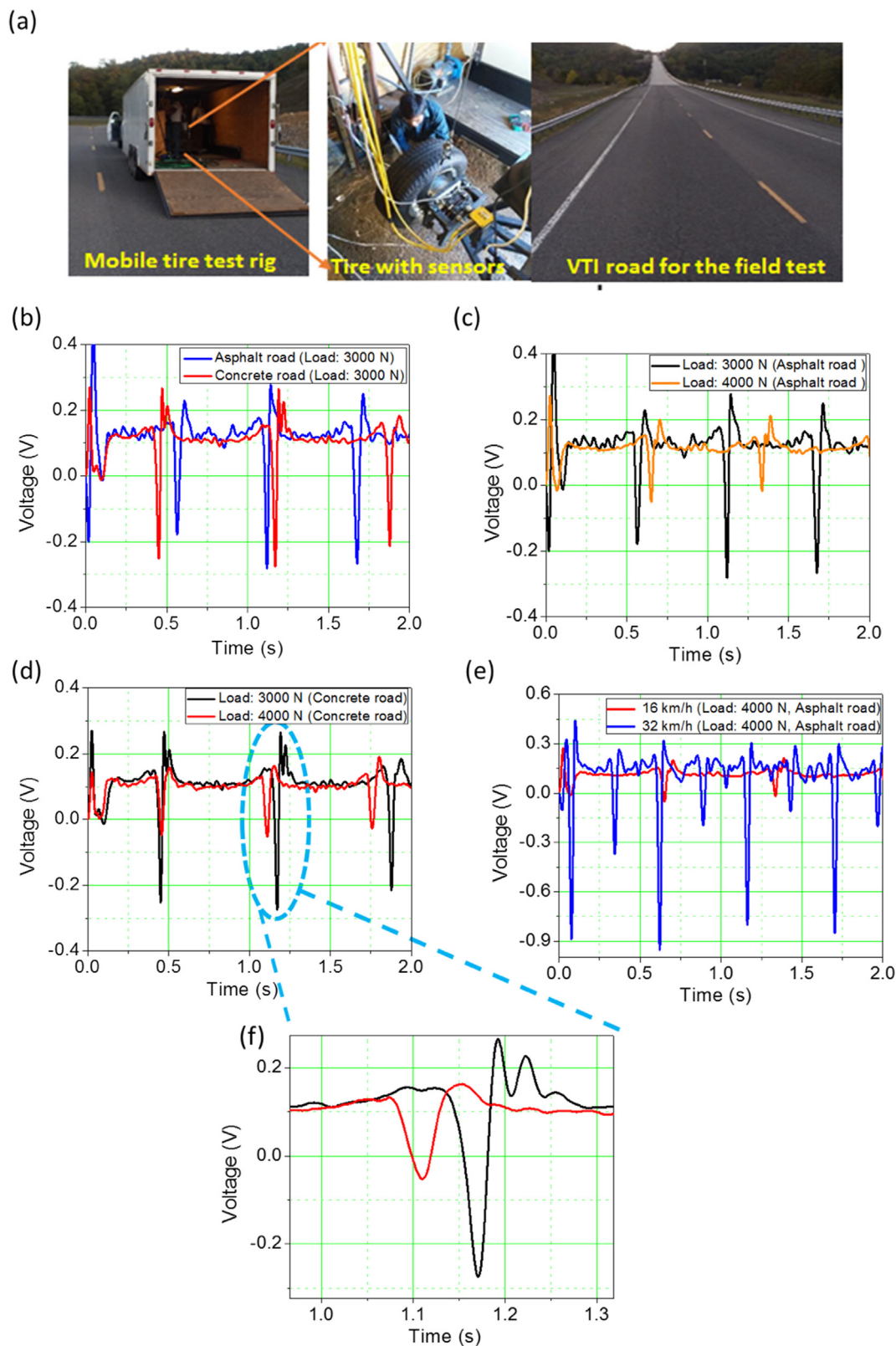


Fig. 8. (a) Test setup for the field experiments. (b)-(d) Waveform generated due to tire deformation at the speed of 16 km/h on different terrain and loads at 193 kPa tire pressure. (e) Comparative waveform change at different speeds of 16 km/h and 32 km/h. (f) Zoomed image of one cycle of waveform having different wheel load.

5. Conclusions

In summary, we demonstrated the feasibility of a self-powered tire sensor based on the piezoelectric effect for the autonomous vehicles. We report a detailed experimental analysis of the sensor-cum-harvester

and its integration with a tire. Theoretical calculations were performed to model the tire-piezoelectric field testing results. The key features of the present work can be summarized as:

- Detailed experimental analysis of polymer-based piezoelectric patch

in the lab environment at different frequencies corresponding to different vehicle speeds. Maximum peak power was evaluated to be $\sim 580 \mu\text{W}$ at 16 Hz.

- Demonstrated the wireless data transfer from the sensor by utilizing the stored energy generated from the piezoelectric patch. The output power was enough to light up 78 LEDs directly. The analysis shows that the power requirement for the wireless data transfer is met using the piezoelectric patch.
- Developed a mathematical model to calculate the radial and tangential displacement of the moving tire, and the generated voltage from the piezoelectric sensor mounted on the tire of the mobile test rig. Our modeling (of real field conditions) results indicated increased voltage output from the sensor (mounted on the tire) with increased vehicle speed.
- Finally, we conducted the field test with the real tire having a piezoelectric sensor, for different parameters, such as different tire speeds, loads and terrains. These field tests indicated no observable change in voltage output (from the sensor) due to change in terrain under the same load. Remarkably, we observed a clear change in the voltage output under varying normal loads and speeds, which were in agreement with our modeling results.

We believe this work is an important milestone in the development of smart tires for the next generation of fully autonomous vehicles.

Acknowledgments

The authors gratefully acknowledge the funding from the NSF I/UCRC program. S.P. would like to acknowledge the funding from the Office of Naval Research through a grant (# N00014-16-1-3043). M.G.K. was supported through the NSF-CREST Grant number HRD 1547771. P.K. was supported through the Office of Naval Research through a grant (# N00014-17-1-2520). R.K. were supported through the NSF (USA) grant (IIP-1035042). D.M. acknowledges NSF (USA) grant (# 1700903). H.-C. S would like to acknowledge the support from the National Research Council of Science & Technology (NST) grant by the Korea government (MSIP) (# CAP-17-04-KRISS) and the Energy Technology Development Project (KETEP) grant funded by the Ministry of Trade, Industry and Energy, Republic of Korea (#2018201010636A).

Appendix A. Supplementary data

Supplementary data to this article can be found online at <https://doi.org/10.1016/j.apenergy.2018.09.183>.

References

- [1] Song H-C, Kumar P, Sriramdas R, Lee H, Sharpes N, Kang M-G, et al. Broadband dual phase energy harvester: Vibration and magnetic field. *Appl Energy* 2018;225:1132–42.
- [2] Agudelo AF, García-Contreras R, Agudelo JR, Armas O. Potential for exhaust gas energy recovery in a diesel passenger car under European driving cycle. *Appl Energy* 2016;174:201–12.
- [3] Jo K, Kim J, Kim D, Jang C, Sunwoo M. Development of autonomous car—Part I: Distributed system architecture and development process. *IEEE Trans Ind Electron* 2014;61:7131–40.
- [4] Litman T. Autonomous vehicle implementation predictions. Victoria Transport Policy Institute 2017.
- [5] Abdelkareem MA, Xu L, Ali MKA, Elagouz A, Mi J, Guo S, et al. Vibration energy harvesting in automotive suspension system: A detailed review. *Appl Energy* 2018;229:672–99.
- [6] Yang Z, Zhou S, Zu J, Inman D. High-performance piezoelectric energy harvesters and their applications. *Joule* 2018.
- [7] Lee H, Taheri S. Intelligent tires? A review of tire characterization literature. *IEEE Intell Transp Syst Mag* 2017;9:114–35.
- [8] Matsuzaki R, Todoroki A. Wireless monitoring of automobile tires for intelligent tires. *Sensors* 2008;8:8123–38.
- [9] Sergio M, Manaresi N, Tartagni M, Canegallo R, Guerrieri R. On a road tire deformation measurement system using a capacitive-resistive sensor. *Smart Mater Struct* 2006;15:1700.
- [10] Eom J, Lee H, Choi B. A study on the tire deformation sensor for intelligent tires. *Int J Precis Eng Manuf* 2014;15:155–60.
- [11] Matsuzaki R, Kamai K, Seki R. Intelligent tires for identifying coefficient of friction of tire/road contact surfaces using three-axis accelerometer. *Smart Mater Struct* 2014;24:025010.
- [12] Choi E. Tire-related factors in the pre-crash phase. Report No DOT HS. 2012;811:617.
- [13] Consortium A. Intelligent tyre for accident-free traffic. Technical Research Centre of Finland (VTT). Tech Rep; 2003.
- [14] Enhancement TR. Accountability, and Documentation (TREAD) Act. Public law. 2000;106:114.
- [15] Kubba AE, Jiang K. A comprehensive study on technologies of tyre monitoring systems and possible energy solutions. *Sensors* 2014;14:10306–45.
- [16] Bowen C, Arafa M. Energy harvesting technologies for tire pressure monitoring systems. *Adv Energy Mater* 2015;5.
- [17] Yilmazoglu O, Brandt M, Sigmund J, Genc E, Hartnagel H. Integrated InAs/GaSb 3D magnetic field sensors for the intelligent tire. *Sens Actuat, A* 2001;94:59–63.
- [18] Doumiati M, Victorino A, Charara A, Lechner D. Lateral load transfer and normal forces estimation for vehicle safety: experimental test. *Veh Syst Dyn* 2009;47:1511–33.
- [19] Braghin F, Brusarosco M, Cheli F, Cigada A, Manzoni S, Mancosu F. Measurement of contact forces and patch features by means of accelerometers fixed inside the tire to improve future car active control. *Veh Syst Dyn* 2006;44:3–13.
- [20] Yi J. A piezo-sensor-based “smart tire” system for mobile robots and vehicles. *IEEE/ASME Trans Mechatron* 2008;13:95–103.
- [21] Erdogan G, Alexander L, Rajamani R. Estimation of tire-road friction coefficient using a novel wireless piezoelectric tire sensor. *IEEE Sens J* 2011;11:267–79.
- [22] Hattori Y. Method for detecting strain state of tire, device for detecting strain state, and the tire. Google Patents 2007.
- [23] Becherer T, Fehrl M. Vehicle wheel provided with a pneumatic tire having therein a rubber mixture permeated with magnetizable particles. Google Patents 1999.
- [24] Todoroki A, Miyatani S, Shimamura Y. Wireless strain monitoring using electrical capacitance change of tire: part I—with oscillating circuit. *Smart Mater Struct* 2003;12:403.
- [25] Matsuzaki R, Todoroki A. Passive wireless strain monitoring of actual tire using capacitance-resistance change and multiple spectral features. *Sens Actuat, A* 2006;126:277–86.
- [26] Pohl A, Ostermayer G, Reindl L, Seifert F. Monitoring the tire pressure at cars using passive SAW sensors. In: *Ultrasonics Symposium, 1997 Proceedings, IEEE; 1997*. p. 471–4.
- [27] Dixon B, Kalinin V, Beckley J, Lohr R. A second generation in-car tire pressure monitoring system based on wireless passive SAW sensors. In: *International Frequency Control Symposium and Exposition, IEEE; 2006*. p. 374–80.
- [28] Ko WH, Wang Q. Touch mode capacitive pressure sensors. *Sens Actuat, A* 1999;75:242–51.
- [29] Pohl A, Steindl R, Reindl L. The “intelligent tire” utilizing passive SAW sensors measurement of tire friction. *IEEE Trans Instrum Meas* 1999;48:1041–6.
- [30] Lee J, Choi B. Development of a piezoelectric energy harvesting system for implementing wireless sensors on the tires. *Energy Convers Manage* 2014;78:32–8.
- [31] Velupillai S, Guven L. Tire pressure monitoring applications of control. *IEEE Control Syst* 2007;27:22–5.
- [32] Gawron JH, Keoleian GA, De Kleine RD, Wallington TJ, Kim HC. Life cycle assessment of connected and automated vehicles: sensing and computing subsystem and vehicle level effects. *Environ Sci Technol* 2018;52:3249–56.
- [33] Singh KB, Bedekar V, Taheri S, Priya S. Piezoelectric vibration energy harvesting system with an adaptive frequency tuning mechanism for intelligent tires. *Mechatronics* 2012;22:970–88.
- [34] Schier M, Nasri M, Kraft W, Kevlishvili N, Paulides JJ, Encica L. Combining mechanical, electrical and thermal energy conversion for ecological vehicle energy harvesting concepts. In: *2018 Thirteenth International Conference on Ecological Vehicles and Renewable Energies (EVER), IEEE; 2018*. p. 1–10.
- [35] Tornincasa S, Repetto M, Bonisoli E, Di Monaco F. Energy harvester for vehicle tires: Nonlinear dynamics and experimental outcomes. *J Intell Mater Syst Struct* 2012;23:3–13.
- [36] Hatipoglu G, Urey H. FR4-based electromagnetic energy harvester for wireless tyre sensor nodes. *Procedia Chem* 2009;1:1211–4.
- [37] Van den Ende D, Van de Wiel H, Groen W, Van der Zwaag S. Direct strain energy harvesting in automobile tires using piezoelectric PZT-polymer composites. *Smart Mater Struct* 2011;21:015011.
- [38] Dudem B, Kim DH, Bharat LK, Yu JS. Highly-flexible piezoelectric nanogenerators with silver nanowires and barium titanate embedded composite films for mechanical energy harvesting. *Appl Energy* 2018;230:865–74.
- [39] Hu Y, Xu C, Zhang Y, Lin L, Snyder RL, Wang ZL. A nanogenerator for energy harvesting from a rotating tire and its application as a self-powered pressure/speed sensor. *Adv Mater* 2011;23:4068–71.
- [40] Zhang H, Yang Y, Zhong X, Su Y, Zhou Y, Hu C, et al. Single-electrode-based rotating triboelectric nanogenerator for harvesting energy from tires. *ACS Nano* 2013;8:680–9.
- [41] Low-Power Sensing. Freescale Semiconductor, Inc; 2015.
- [42] Tire Pressure Monitoring (TPM) System. 2009 Microchip Technology Inc.; 2009.
- [43] Gomez C, Oller J, Paradells J. Overview and evaluation of bluetooth low energy: an emerging low-power wireless technology. *Sensors* 2012;12:11734.
- [44] Siekkinen M, Hienkari M, Nurminen JK, Nieminen J. How low energy is bluetooth low energy? Comparative measurements with ZigBee/802.15.4. *2012 IEEE Wireless Communications and Networking Conference Workshops (WCNCW) 2012*. p. 232–7.
- [45] Police: Flat tire leads to deadly crash on I-70; thousands of gallons of oil spilled.

- FOX59 WEB; 2017.
- [46] Preumont A. *Mechatronics: dynamics of electromechanical and piezoelectric systems*. Springer Science & Business Media; 2006.
- [47] Sunrong G. *A study of in-plane dynamics of tires*. Delft University of Technology, The Netherlands PhD Dissertation. 1993.
- [48] Wei Y, Nasdala L, Rothert H. Analysis of forced transient response for rotating tires using REF models. *J Sound Vib* 2009;320:145–62.
- [49] Xiong Y, Tuononen A. The in-plane deformation of a tire carcass: analysis and measurement. *Case Stud Mech Syst Signal Process* 2015;2:12–8.
- [50] Parks VJ, Durelli A. Various forms of the strain-displacement relations applied to experimental strain analysis. *Exp Mech* 1964;4:37–47.
- [51] Meirovitch L. A modal analysis for the response of linear gyroscopic systems. *J Appl Mech* 1975;42:446–50.
- [52] On Tsotras A. *the interaction between modal behaviour and shear force behaviour of a pneumatic tyre*: ©. Achillefs Tsotras 2010.